

Effect of quantum fluctuations on structural phase transitions in SrTiO_3 and BaTiO_3

W. Zhong and David Vanderbilt

Department of Physics and Astronomy, Rutgers University, Piscataway, New Jersey 08855-0849

(Received 20 September 1995)

Using path-integral Monte Carlo simulations and an *ab initio* effective Hamiltonian, we study the effects of quantum fluctuations on structural phase transitions in the cubic perovskite compounds SrTiO_3 and BaTiO_3 . We find quantum fluctuations affect ferroelectric (FE) transitions more strongly than antiferrodistortive (AFD) ones, even though the effective mass of a single FE local mode is larger. For SrTiO_3 we find that the quantum fluctuations suppress the FE transition completely, and reduce the AFD transition temperature from 130 to 110 K. For BaTiO_3 , quantum fluctuations do not affect the order of the transition, but do reduce the transition temperature by 35–50 K. The implications of the calculations are discussed.

Quantum fluctuations typically have a very important effect on the structural and thermodynamic properties of materials consisting of light atoms like hydrogen and helium. For example, quantum effects introduce large corrections to the calculated hydrogen density distribution in the Nb:H system.¹ For materials with heavier atoms, however, the quantum fluctuation can have only a small effect on the distribution of atomic displacements, and thus typically do not have a noticeable effect on the structural and thermodynamic properties of the material. However, exceptions may occur. As we shall see, the cubic perovskites can exhibit decisive quantum-fluctuation effects, despite the fact that the lightest constituent is oxygen. This can occur because these materials have several competing structures with very small structural and energetic differences.²

A good example is SrTiO_3 . While it has the simple cubic perovskite structure at high temperature, SrTiO_3 goes through an antiferrodistortive (AFD) transition at 105 K to a tetragonal phase in which the oxygen octahedra have rotated in opposite senses in neighboring unit cells. The observed softening of the ferroelectric (FE) polar phonons with further reduction of temperature in the range 50–100 K would appear to extrapolate to a FE transition close to 20 K, but instead the softening saturates and no such transition is observed.³ The absence of a true FE transition is suggested to be suppressed by quantum fluctuations, giving rise to a “quantum paraelectric” phase at very low temperature.⁴ Some experiments appear to suggest a sharp transition to this low-temperature phase at about 40 K, perhaps indicating the formation of some kind quantum coherent state.^{5,6} However, until a plausible candidate for the order parameter of the low-temperature phase is put forward, these ideas must remain highly speculative.

These developments have stimulated many theoretical efforts to understand the quantum effects in SrTiO_3 .^{4,7–9} However, the previous work has all been qualitative or empirical in approach. Although it was shown that quantum zero-point motion is capable of suppressing phase transitions,⁹ a detailed microscopic approach is needed to gain a quantitative and detailed understanding of the quantum effects at finite temperature. Recently, an *ab initio* effective-Hamiltonian scheme has been developed to study structural phase transitions of cubic perovskites. It has been successfully applied to

BaTiO_3 (Refs. 10 and 11) and SrTiO_3 ,^{12,13} giving good agreement with experimental observations. Treating atomic motion classically, it predicted FE phase transitions for SrTiO_3 at low temperature, thus giving indirect support for the notion that quantum fluctuations (not included in the theory) must be responsible for the observed absence of a low-temperature FE phase.

In the present work, we have extended the previous treatment of the first-principles based effective Hamiltonian to include quantum fluctuations. In particular, we use path-integral (PI) quantum Monte Carlo simulations to study the effect of quantum fluctuations on the structural phase transitions in SrTiO_3 and BaTiO_3 . For SrTiO_3 , we find that the quantum fluctuations have only a modest effect on the AFD transition temperature, while the FE transition is suppressed entirely. We discuss the relative importance of AFD and FE quantum fluctuations in some detail, and examine the potential implications of our results for understanding the low-temperature behavior of the material. For BaTiO_3 , in which the FE transitions occur at higher temperature, we find that the quantum effects are less dramatic.

We start by reviewing the effective Hamiltonian and its construction. Two approximations are involved. First, since both the FE and AFD transitions involve only small structural distortions, we represent the energy surface by a Taylor expansion around the high-symmetry cubic perovskite structure, including up to fourth-order anharmonic terms. Second, because only low-energy distortions are important to the structural properties, we include only three such distortions in our expansion: the soft FE mode, the AFD mode, and an elastic mode. These are represented, respectively, by local-mode amplitudes \mathbf{f}_i , \mathbf{a}_i , and \mathbf{u}_i , where i is a cell index. The local modes are constructed in such a way that a uniform (or, for AFD, a uniformly staggered) arrangement of the mode vectors represents the desired low-energy excitation.¹¹ Thus, we work with local-mode vectors instead of atomic displacements. This reduces the number of degrees of freedom from 15 to 9 per cell and greatly reduces the complexity of the Taylor expansion. The Hamiltonian is specified by a set of expansion parameters determined using highly accurate first-principles calculations with Vanderbilt ultrasoft pseudopotentials.¹⁴ The details of the Hamiltonian, the first-

principles calculations, and the values of the expansion parameters have been reported elsewhere.^{10–13}

In our previous work, we have used this effective Hamiltonian by applying Monte Carlo simulation techniques to study the thermodynamics of the system in the classical limit. Assuming the ionic motions are classical is usually a good approximation for systems such as cubic perovskites containing atoms no less massive than oxygen. However, the structural differences and energy barriers between the cubic structure and the possible (rhombohedral or tetragonal) distorted structures are very small. A rough estimate of the importance of quantum fluctuations can be obtained from the Heisenberg uncertainty principle $\Delta p \cdot \Delta q \geq \hbar/2$, or equivalently,

$$\Delta E \geq \hbar^2 / (8m\Delta q^2). \quad (1)$$

Here, Δq denotes the uncertainty in the structural coordinate, which is related to the structural difference between phases. ΔE is the energy uncertainty, or zero-point energy, which may prevent the occurrence of the distorted phase if it is larger than the classical free-energy reduction. So if the structural and energetic differences between phases are small enough, quantum suppression may occur even for fairly massive ions. For a quantitative understanding, we need to perform statistical simulations that treat the ionic motion quantum mechanically.

Here, we adopt the path-integral (PI) technique¹⁵ of quantum simulations, which has proven to be a very successful method for studying H- and He-related systems.^{1,16} The method is based on Feynman's PI formulation of quantum mechanics.¹⁷ This formulation states that the partition function of the original quantum-statistical systems of particles can be approximated by the partition function of P subsystems of classical particles with each quantum particle replaced by a cyclic chain of P beads coupled by harmonic springs. Each subsystem (comprising one bead from each chain) has internal interactions identical to the reference classical system, except for a reduction in strength by a factor $1/P$. The spring constant of the harmonic springs coupling the beads inside a certain cyclic chain is $mP/\hbar^2\beta^2$, where m is the mass of the quantum particle and β the inverse temperature $(k_B T)^{-1}$. This approximation becomes exact when the number of beads $P \rightarrow \infty$, but in practice almost exact results can be obtained with a finite P depending on the system of interest. This way, thermodynamic properties of the N -particle quantum system can be obtained from the study of a $(P \times N)$ -particle classical system.

The only extra inputs we need are the masses of all the "particles" in our system. The degrees of freedom in our Hamiltonian are the three local-mode amplitude vectors \mathbf{f}_i , \mathbf{a}_i , and \mathbf{u}_i associated with each unit cell i . Each local mode involves displacements of several ions. If we regard each local vector as representing the displacement of some "pseudoparticle," the mass of each such pseudoparticle can be determined from all the ionic displacements involved. Since two local-mode vectors may involve the same ion, we actually have a nondiagonal mass matrix. For example, the mass matrix elements between local modes \mathbf{f}_i and \mathbf{f}_j , or equivalently, $f_{i\alpha}$ and $f_{j\beta}$, can be constructed through

$$m_{i\alpha,j\beta} = \xi(i\alpha) \cdot M \cdot \xi(j\beta). \quad (2)$$

Here, i and j are the cell indices, while α and β denote Cartesian components. $\xi(i\alpha)$ is the eigenvector describing atomic displacements associated with local mode $f_{i\alpha}$, and M is a (diagonal) mass matrix in the $15L^3$ -dimensional space of atomic displacements of our $L \times L \times L$ supercell. Similarly, mass matrix elements connecting different kinds of local vectors, such as those between \mathbf{f}_i and \mathbf{a}_i , are also included. The entire mass matrix can be calculated once and for all, and the extension of the PI technique to handle a nondiagonal mass matrix is straightforward.

The study of the thermodynamic properties of the classical system is performed using Monte Carlo (MC) simulations.¹⁸ The original simulation cell is an $L \times L \times L$ cube, with three vectors \mathbf{f}_i , \mathbf{a}_i , and \mathbf{u}_i at each lattice point i . Periodic boundary conditions are used, and homogeneous strains of the entire supercell are included. Each local vector is converted to a string of P beads, so that we have $9PL^3$ degrees of freedom per simulation supercell. We use a single-flip algorithm, making trial moves of the vectors at each site in turn and testing acceptance after each move. We say that one Monte Carlo sweep (MCS) has been completed when all vectors on all sites have been tried once. Because of the 1% lattice-constant error in our local-density approximation (LDA) calculations and the strong sensitivity of the structural transitions to the lattice constant, all our simulations are performed at a negative pressure to restore the experiment lattice constant, as in our previous work.^{10–13}

The Trotter number P should be large enough to ensure that the quantum effects are correctly accounted for. On the other hand, the computational load increases rapidly with increasing P , because of both larger system size and longer correlation time with larger P . In our simulation, the proper Trotter number for each temperature is chosen empirically. For a certain temperature, we simulate systems with increasing Trotter number $P=1, 2, 4, 8, 16, \dots$. We equilibrate systems with each P and monitor their order parameters. We determine that the P is large enough if the monitored quantities converge. If a certain quantity is sensitive to P , its value at $P=\infty$ can be extrapolated following the formula $a_0 + a_1/P + a_2/P^2$ (Ref. 19).

We concentrate on SrTiO₃ and study the effect of quantum fluctuation on both FE and AFD phase transitions. In Fig. 1, we show the FE and AFD order parameters $\mathbf{f}(\Gamma)$ and $\mathbf{a}(R)$ as a function of temperature for a $12 \times 12 \times 12$ simulation cell. The classical data (previously published in Ref. 12) are produced by a cooling-down simulation, starting at 250 K and cooling down gradually, equilibrating and then simulating to obtain the order parameters.¹² The quantum simulations are performed with $P=4$, which is found to give converged results for $T > 60$ K and qualitatively correct results for $T > 20$ K. We use the equilibrium configuration from the classical simulations ($P=1$) as the starting configuration. We find the system reaches equilibrium faster this way than it does if gradually cooled and the results are less affected by hysteresis. The system is equilibrated for 10 000 MCS's, and then another 30 000–70 000 MCS's are used to obtain the reported thermodynamic averages.

Figure 1 shows that the quantum fluctuations do affect both the AFD and FE phase transitions. The AFD phase transition temperature decreases from 130 K to 110 K when the quantum fluctuations are turned on, bringing the results into

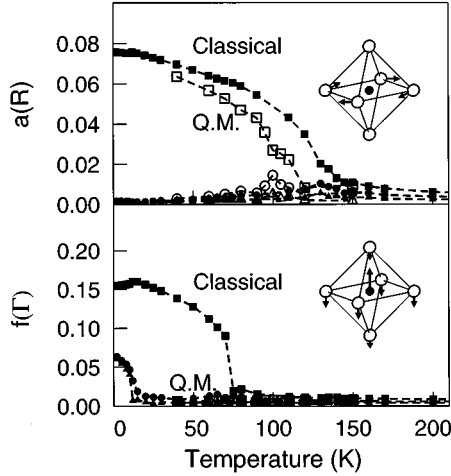


FIG. 1. AFD and FE order parameters $\mathbf{a}(R)$ and $\mathbf{f}(\Gamma)$ as a function of temperature for a $12 \times 12 \times 12$ SrTiO₃ simulation cell. Squares, circles, and triangles indicate the largest, intermediate, and smallest components of the order parameter, respectively. Filled symbols are from classical simulations, while open symbols are from path-integral simulations with $P=4$ (the latter for the FE case are nearly zero and are thus not very visible). Insets indicate schematically the nature of the AFD and FE distortions.

better agreement with the experimental result of 105 K. On the other hand, the quantum fluctuations can be seen to have completely suppressed the FE phase transitions, at least down to 40 K. Further simulations going as high as $P=20$ place an upper bound of about 5 K on any possible FE phase transition temperature. Thus, we conclude that quantum fluctuations almost certainly suppress the FE phase transitions completely, resulting in a paraelectric phase down to $T=0$.

Since the effect of quantum fluctuations is more dramatic on the FE transitions, we analyze this case in more detail. In the paraelectric phase, the fluctuation of the FE local-mode vector \mathbf{f} has both quantum and thermal contributions. We identify the thermal fluctuations as those associated with the fluctuations of the center of gravity of the cyclic chain. More specifically, letting $\mathbf{f}(i, s, t)$ represent \mathbf{f} on lattice site i , Trotter slice s , and MCS t , the thermal fluctuation can be obtained from our simulation using

$$(\Delta f^{\text{thermal}})^2 = \langle \langle f_s^2 \rangle \rangle_{i,t}, \quad (3)$$

while the total fluctuation is

$$(\Delta f^{\text{total}})^2 = \langle f^2 \rangle_{i,s,t}. \quad (4)$$

Here the brackets represent the indicated average. The part of fluctuation due solely to the quantum effects can be obtained from $(\Delta f^{\text{QM}})^2 = (\Delta f^{\text{total}})^2 - (\Delta f^{\text{thermal}})^2$. The result for a $10 \times 10 \times 10$ lattice is shown in Fig. 2. The results are obtained from simulations at several small Trotter numbers and then extrapolated to $P=\infty$ using the formula $a_0 + a_1/P + a_2/P^2$. As expected, the thermal fluctuation decrease with decreasing temperature, while the quantum fluctuations increase. Below 70 K, the quantum fluctuations dominate.

Recent experiments suggest there may be a weak signature of a phase transition in SrTiO₃ around 40 K.⁵ This was

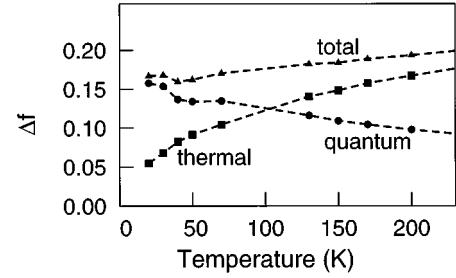


FIG. 2. Classical (squares), quantum (circles), and total (triangles) RMS fluctuation of the FE local-mode vectors [Eqs. (3) and (4)] in SrTiO₃ as a function of temperature.

tentatively suggested to be a phase transition to a coherent quantum state in which small FE domains propagate through the crystal. Because the size of our simulation cell is much smaller than the domain size suggested, we expect that such a state would appear as a real FE phase in our simulation. This is not observed. However, our simulation does reveal some changes in the character of the FE fluctuations at low temperature. A typical FE fluctuation at high temperature resembles the soft eigenvector of the force-constant matrix, which is independent of the masses, since the classical thermodynamic properties are related only to the potential energy. However, the quantum fluctuations are quite sensitive to the ionic masses, and at low temperature the fluctuations of light (primarily oxygen-related) degrees of freedom are accentuated. This crossover in the character of the fluctuations occurs gradually below 100 K, and we suspect that it might possibly be responsible for the experimentally observed anomalies which were interpreted in terms of a phase transition. If this is the case, the “quantum paraelectric” phase at very low temperature is probably not separated by a true phase transition from the classical paraelectric phase at higher temperature.

To better characterize the impact of the quantum effects on FE transitions, we also apply the PI simulations to BaTiO₃. The results are summarized in Table I. The simulation procedure is the same as for SrTiO₃, except that the AFD degrees of freedom are neglected in BaTiO₃ because of their high energy. Experimentally, BaTiO₃ has four phases in the sequence cubic (C), tetragonal (T), orthorhombic (O), and rhombohedral (R) with decreasing temperature. Our classical simulations correctly reproduce this transition sequence, and give transition temperatures that are in reasonable agreement with (~ 15 – 30% below) the experimental ones. We have argued previously that the quantitative discrepancy can probably be traced to the LDA lattice-constant

TABLE I. The effect of quantum fluctuations on the FE transition temperatures in BaTiO₃, for a $12 \times 12 \times 12$ supercell. R , O , T , and C indicate rhombohedral, orthorhombic, tetragonal, and cubic phases, respectively.

Phase	Classical	Quantum	Expt.
$O-R$	200 ± 10	150 ± 10	183
$T-O$	232 ± 2	195 ± 5	278
$C-T$	296 ± 1	265 ± 5	403

error.^{10,11} Here, we find that, with quantum effects included, the calculated transition sequence is still the same, while the transition temperatures are reduced further by 35 to 50 K. Although the absolute transition temperatures are thus in slightly worse agreement with experiment, the spacing between phases is more reasonable. In any case, it is clear that the quantum effects can have a substantial effect on the FE transition temperatures even up to several hundreds of degrees K, a result which was not obvious from the outset.

It may appear counterintuitive that quantum effects on the FE instability are much stronger than on the AFD instability in SrTiO₃. After all, the AFD instability involves only the motion of oxygen atoms, while the FE instability involves mainly Ti atoms which are three times heavier than the oxygen atoms. A partial explanation can be drawn from the fact that the structural change involved in the FE distortion (0.1 a.u. for Ti in SrTiO₃) is much smaller than for the AFD distortion (0.3 a.u. for O). As a result, $m\Delta q^2$ turns out to be three times larger for the AFD case, even though the effective mass is smaller. Thus, according to Eq. (1), the effect of the quantum fluctuations will be less significant for the AFD case.

We think a more fundamental explanation may be found in the stronger spatial correlations between AFD distortions. In the cubic phase, the spatial correlations for the FE local vectors are chainlike or quasi-one-dimensional (1D): $f_z(\mathbf{R}_i)$ correlates strongly only with $f_z(\mathbf{R}_i \pm n\hat{z})$, where n is a small integer number and a is the lattice constant.^{20,13} This correlation is due to the strong Coulomb interactions between FE local modes,²¹ which strongly suppress longitudinal excitations relative to transverse ones. With the correla-

tion length estimated at $10a$,¹³ we can roughly say that about ten local-mode vectors are “bound together” and the effective mass becomes ten times larger. On the other hand, the AFD modes, associated with rotation of the oxygen octahedral, correlate strongly with each other because of the rigidity of the octahedral unit. The correlation region is 2D disc-like: $a_z(\mathbf{R}_i)$ correlates strongly with $a_z(\mathbf{R}_i \pm na\hat{x} + ma\hat{y})$, where m is again a small integer. The AFD correlation length is comparable with the FE one,¹³ but now the 2D nature implies that roughly 100 mode vectors are tied together, for a mass enhancement of 100 instead of just 10. Thus, this effect weakens the quantum fluctuations much more for the AFD than for the FE case, and one should generally expect quantum suppression of phase transitions to be stronger in the FE case.

In summary, we have applied the PI technique to study the effect of quantum fluctuations on FE and AFD phase transitions in SrTiO₃ and BaTiO₃. We find that the quantum fluctuations have a weaker effect on the AFD transition than on the FE one, because the AFD modes are more strongly correlated with each other. In the case of SrTiO₃, we find that the FE phase is suppressed entirely, thereby supporting the notion of “quantum paraelectric” behavior (though not necessarily a distinct phase) at very low temperature. The AFD transition temperature is found to be only slightly reduced. For BaTiO₃, we find that the quantum effects preserve the transition sequence and reduce the transition temperatures modestly.

This work was supported by ONR Grant No. N00014-91-J-1184.

-
- ¹M. J. Gillan, Phys. Rev. Lett. **58**, 563 (1987).
²M. E. Lines and A. M. Glass, *Principles and Applications of Ferroelectrics and Related Materials* (Clarendon, Oxford, 1977).
³R. Viana *et al.*, Phys. Rev. B **50**, 601 (1994).
⁴K.A. Müller and H. Burkard, Phys. Rev. B **19**, 3593 (1979).
⁵K.A. Müller, W. Berlinger, and E. Tosatti, Z. Phys. B **84**, 277 (1991).
⁶R. Vacher *et al.*, Europhys. Lett. **17**, 45 (1992); O. M. Nes, K. A. Müller, T. Suzuki, and F. Fossheim, *ibid.* **19**, 397 (1992); E. V. Balashova *et al.*, Solid State Commun. **94**, 17 (1995).
⁷R. Martonak and E. Tosatti, Phys. Rev. B **49**, 12 596 (1994).
⁸J. H. Barrett, Phys. Rev. **86**, 118 (1952).
⁹T. Schneider, H. Beck, and E. Stoll, Phys. Rev. B **13**, 1123 (1976).
¹⁰W. Zhong, D. Vanderbilt, and K. M. Rabe, Phys. Rev. Lett. **73**, 1861 (1994).
¹¹W. Zhong, D. Vanderbilt, and K. M. Rabe, Phys. Rev. B **52**, 6301 (1995).
¹²W. Zhong and D. Vanderbilt, Phys. Rev. Lett. **74**, 2587 (1995).
¹³W. Zhong and D. Vanderbilt (unpublished).
¹⁴D. Vanderbilt, Phys. Rev. B **41**, 7892 (1990).
¹⁵J. Barker, J. Chem. Phys. **70**, 2914 (1979); D. Chandler and P. G. Wolynes, *ibid.* **74**, 7 (1981); *Monte Carlo Methods in Quantum Problems*, edited by M. H. Kalos (Reidel, Dordrecht, 1984).
¹⁶D. Ceperley, Rev. Mod. Phys. **67**, 279 (1995); E. Kaxiras and Z. Guo, Phys. Rev. B **49**, 11 822 (1994).
¹⁷R. P. Feynman, *Statistical Mechanics* (Benjamin, Reading, MA, 1972).
¹⁸M. P. Allen and D. J. Tildesley, *Computer Simulation of Liquids* (Oxford, New York, 1990); *The Monte Carlo Method in Condensed Matter Physics*, edited by K. Binder (Springer-Verlag, Berlin, 1992).
¹⁹A. Cuccoli *et al.*, Phys. Rev. B **51**, 12 369 (1995).
²⁰R. Yu and H. Krakauer, Phys. Rev. Lett. **74**, 4067 (1995).
²¹W. Zhong, R. D. King-Smith, and D. Vanderbilt, Phys. Rev. Lett. **72**, 3618 (1994).